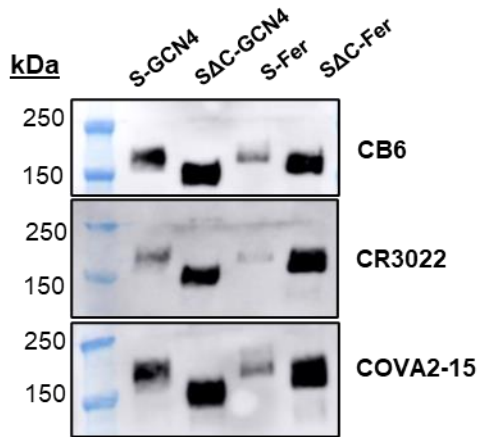


Supplemental Information

Table of contents:

- **Figure S1.** Spike ferritin nanoparticles are expressed at levels similar to those of spike GCN4 trimers.
- **Figure S2.** Size-exclusion chromatography multi-angle light scattering molecular weight determination of spike ferritin nanoparticles and analysis of other antigens.
- **Figure S3.** Cryo-EM of S-Fer and S Δ C-Fer nanoparticles confirms the presence of spike proteins displayed on the surface of ferritin.
- **Figure S4.** SARS-CoV-2 antigens bind to conformation-specific mAbs with similar k_{on} values and do not show non-specific binding.
- **Figure S5.** ELISA confirms that the ACE2 binding site and mAb epitopes are displayed on spike ferritin similarly to their display in the RBD and spike trimers.
- **Figure S6.** Validation of a SARS-CoV-2 neutralization assay using a spike-pseudotyped lentivirus.
- **Table S1.** Mean ELISA binding titers, % ACE2 blocking, and spike-pseudotyped lentivirus neutralization titers from antigen groups at day 21 and day 28 post immunization.
- **Table S2.** Statistical analysis of spike and RBD ELISA titers from day 21 and day 28 immunization timepoints.
- **Table S3.** Statistical analysis of spike and RBD neutralization titers from day 21 and day 28 immunization timepoints.
- **Figure S7.** Sera from mice immunized with SARS-CoV-2 block ACE2 binding to RBD, as indicated by ELISA.
- **Figure S8.** Immunization with SARS-CoV-2 antigens adjuvanted with Quil-A/MPLA leads to robust RBD-specific IgG1 and IgG2 isotype responses and minimal levels of IgM following two doses.
- **Figure S9.** Off-target antibody responses to either *H. pylori* ferritin or GCN4-trimerization domain are similar between ferritin and trimer immunization groups.
- **Figure S10.** Immunization with S Δ C-Fer leads to a dose-dependent neutralizing antibody response and elicits neutralizing antibody levels that are stable up to 20 weeks post immunization.

A



B

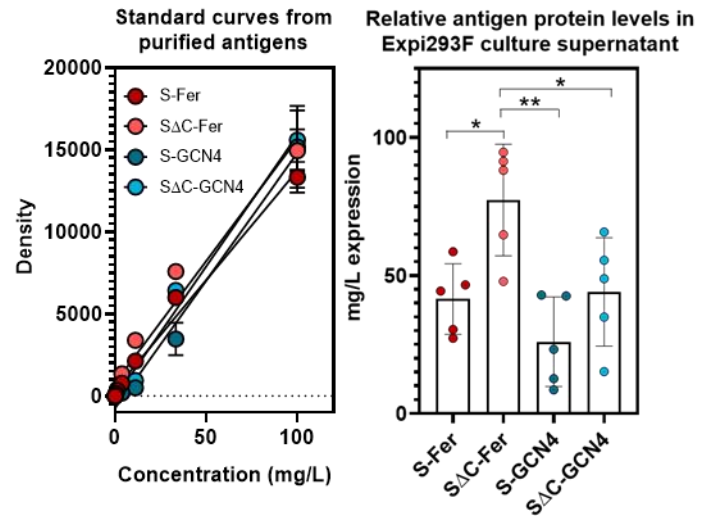
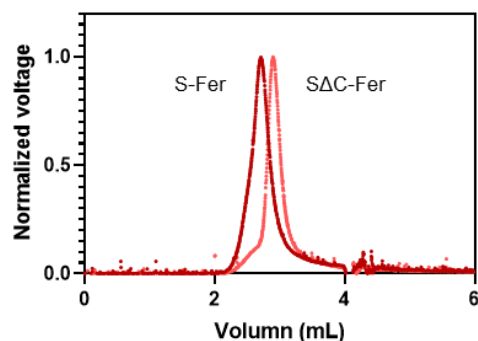


Figure S1. Spike ferritin nanoparticles are expressed at levels similar to those of spike GCN4 trimers. (A) Western blot analysis of Expi293F culture supernatant indicates that expression levels are similar among the spike antigen constructs. Supernatants were blotted with CB6 (top), CR3022 (middle), or COVA2-15 (bottom) SARS-CoV-2 mAbs and read out using an anti-human HRP secondary. (B) Dot blot analysis was performed to estimate protein levels of spike antigens in culture supernatants. Purified antigens were used to generate standard curves using a 3-fold dilution series starting at 0.1 mg/mL (59). Dots were quantified using CR3022 primary mAb followed by anti-human HRP secondary. Standard curves were then used to calculate the amount of protein in harvested culture supernatants from 5 replicate protein expressions. The height of the bar is the mean protein concentration from 5 individual protein expression replicates (points) from culture supernatant; error bars represent the standard deviation. Statistical comparison of expression levels was performed using ordinary one-way ANOVA followed by Tukey's multiple comparisons test. All p values are represented as followed: * = $p \leq 0.05$, ** = $p \leq 0.01$, *** = $p \leq 0.001$, **** = $p \leq 0.0001$

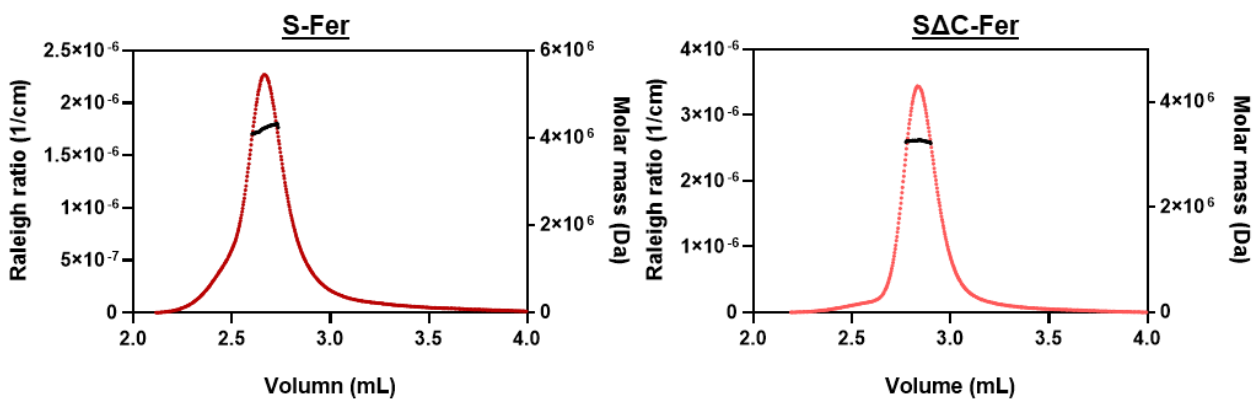
A

SRT SEC-1000 light scattering analysis of spike ferritin particles following freezing



B

Spike ferritin construct	SEC-MALS determined molecular weight (Da)	Predicted molecular weight based on amino acid sequence (Da)
S-Fer	$4.2 \pm 0.17 \times 10^6$	3.7×10^6
SΔC-Fer	$3.1 \pm 0.24 \times 10^6$	3.5×10^6



C

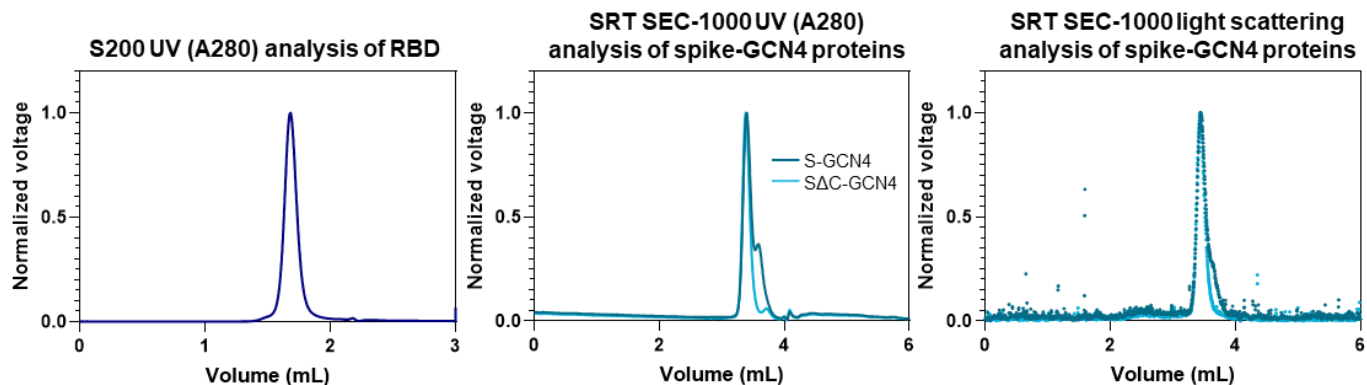


Figure S2. Size-exclusion chromatography multi-angle light scattering molecular weight determination of spike ferritin nanoparticles and analysis of other antigens. (A) Light scattering analysis of the S-Fer and S Δ C-Fer particles on the SRT SEC-1000 analytical column indicate that particles do not aggregate following a freeze-thaw cycle. Glycerol (10%) was added to particle samples prior to snap-freezing. (B) Molecular weight calculation for S-Fer and S Δ C-Fer determined by SEC-MALS was performed with ASTRA software using light scattering and refractive index signals for the particles. The average calculated molecular weight obtained from two independent protein preparations for each particle (S-Fer and S Δ C-Fer) is shown. The expected molecular weight was determined by the amino acid sequence for the individual S-Fer and S Δ C-Fer protomers and multiplied by 24 to account for the number of protomers in a particle. The expected mass does not account for glycosylation; each protomer contains ~20 predicted N-linked glycans which could add up to 1 MDa to the mass of the particle (61). Discrepancies in calculated and expected molecular weights could in part be due to incomplete glycosylation. The plots show a representative curve from each analysis. The colored traces correspond to the left y-axis which shows the Rayleigh ratio, a measure of light scattering. The black line on each peak is the calculated molecular weight, plotted on the right y-axis, as a function of particle elution. This demonstrates that the molecular weight calculation is not subject to variations resulting from artifacts in the eluted peak. (C) SEC-MALS traces for the RBD, S-GCN4, and S Δ C-GCN4 demonstrating that samples are pure and do not form aggregates. Only UV A280 is shown for the RBD because it is too small for light scattering to be detected with the miniDAWN detector.

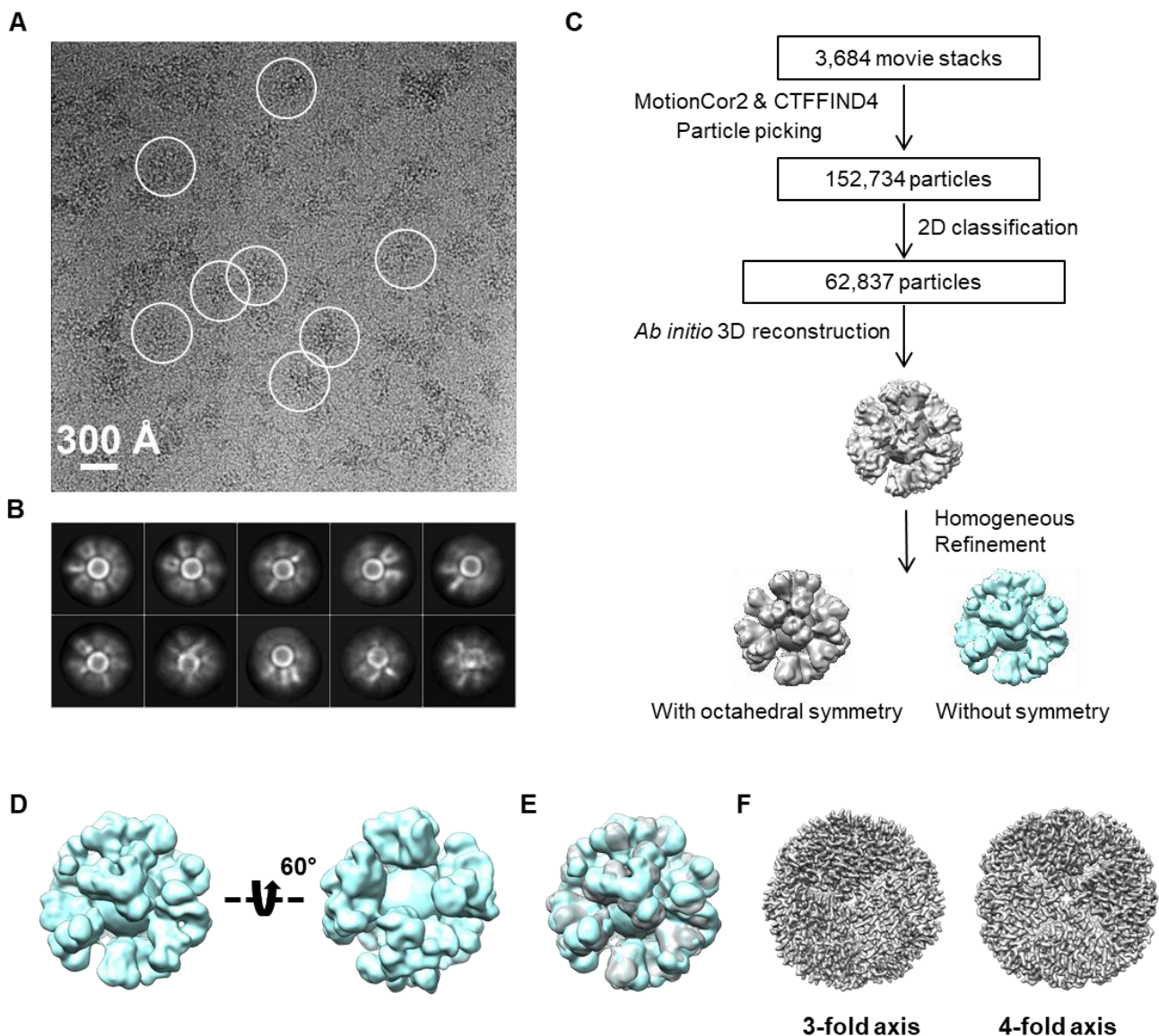


Figure S3. Cryo-EM of S-Fer and S Δ C-Fer nanoparticles confirms the presence of spike proteins displayed on the surface of ferritin. (A) Representative motion-corrected cryo-EM micrograph of S-Fer with particles circled in white. (B) Reference-free 2D class averages of S-Fer nanoparticles from analysis of S-Fer indicating the presence of spike on the surface of the particles. (C) Workflow of cryo-EM data processing of S Δ C-Fer. (D) Reconstructed cryo-EM map of the S Δ C-Fer without symmetry applied (two views). (E) Superimposition (cyan and gray) of the two 3D reconstructions of S Δ C-Fer with and without octahedral symmetry demonstrate that the two maps have high similarity, with a cross-correlation coefficient of 0.99. (F) Single-particle analysis focused on the ferritin core from the S Δ C-Fer dataset. The 3.7-Å resolution reconstructed cryo-EM map is shown in two different views. Left, 3-fold view; Right, 4-fold view.

A

Antigen	Monomer (nM)	Trimer / nanoparticle (nM)	CB6 IgG k_{on} ($M^{-1} s^{-1}$)	COVA2-15 IgG k_{on} ($M^{-1} s^{-1}$)	CR3022 IgG k_{on} ($M^{-1} s^{-1}$)
S-Fer	100	4.2	$5.9 \pm 0.34 \times 10^5$	$5.4 \pm 1.1 \times 10^5$	$4.9 \pm 4.0 \times 10^5$
S Δ C-Fer	100	4.2	$9.9 \pm 3.8 \times 10^5$	$1.1 \pm 0.32 \times 10^6$	$7.3 \pm 5.3 \times 10^5$
S-GCN4	100	33.3	$4.1 \pm 1.1 \times 10^5$	$4.3 \pm 0.80 \times 10^5$	$2.3 \pm 0.42 \times 10^5$
S Δ C-GCN4	100	33.3	$4.1 \pm 0.16 \times 10^5$	$4.9 \pm 0.081 \times 10^5$	$2.3 \pm 0.073 \times 10^5$
RBD	100	--	$1.9 \pm 0.16 \times 10^5$	$4.9 \pm 0.66 \times 10^5$	$3.2 \pm 0.70 \times 10^5$

B

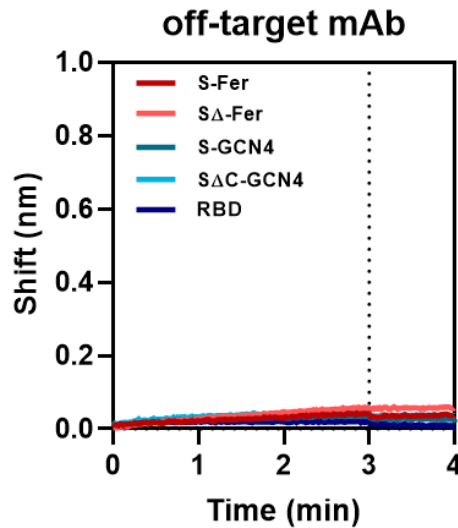


Figure S4. SARS-CoV-2 antigens bind to conformation specific mAbs with similar k_{on} values and do not show non-specific binding. (A) Binding curves shown in Figure 3D were fit with a non-linear association/dissociation equation to obtain kinetic binding parameters. Several binding interactions did not have quantifiable off-rates and thus k_{on} values are presented as a comparative measure of each mAb binding to each antigen in the panel. (B) BLI shows that antigens do not bind non-specifically to an off-target Ebola-specific monoclonal antibody, ADI-15731, confirming the specificity of observed binding shown in Figure 3D.

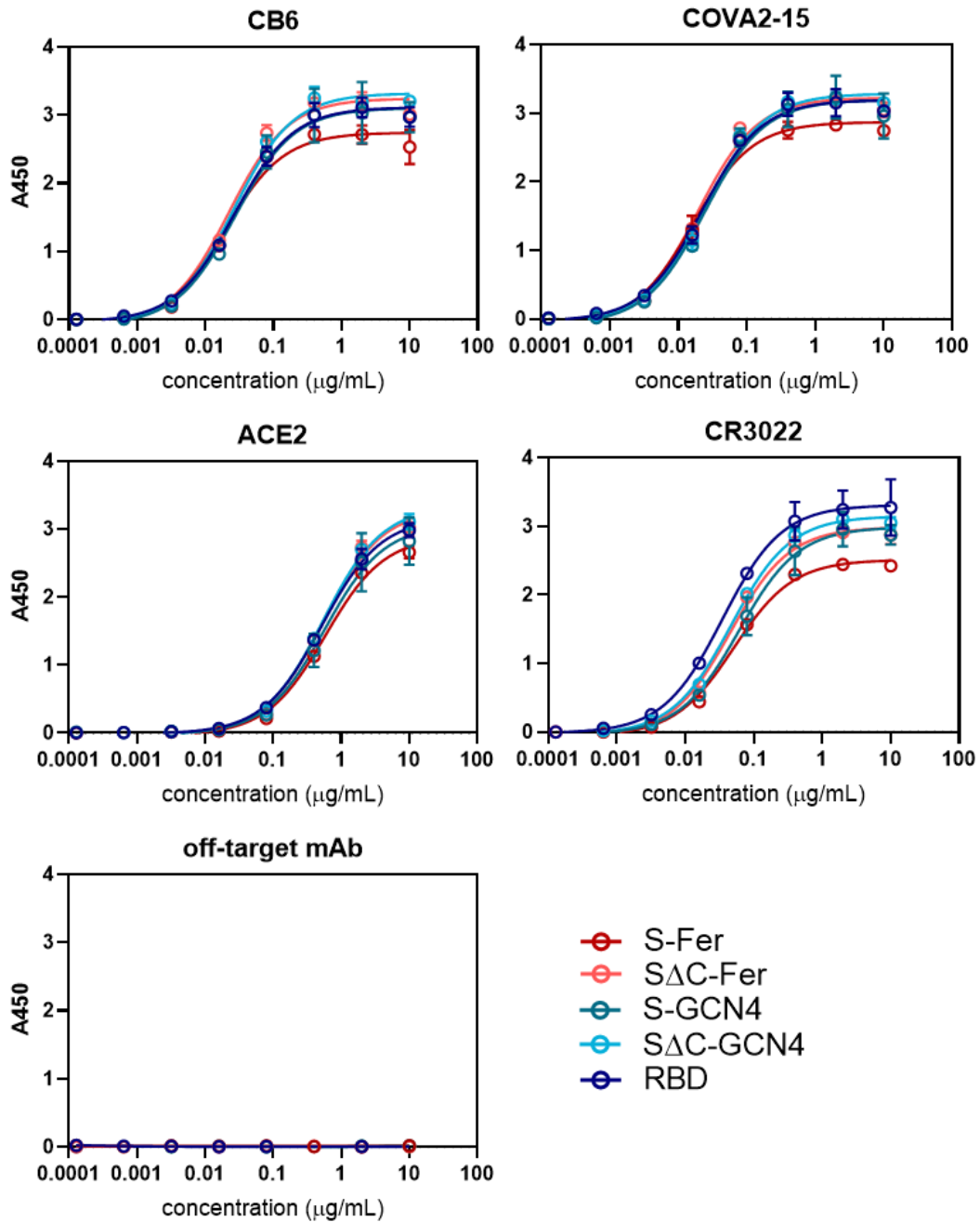
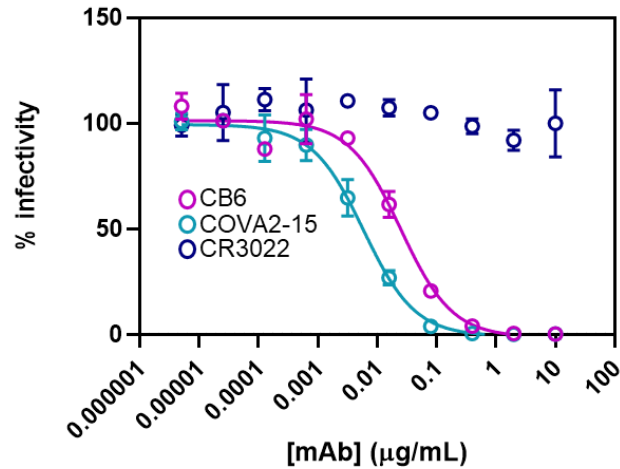


Figure S5. ELISA confirms that the ACE2 binding site and mAb epitopes are displayed on spike ferritin similarly to their display in the RBD and spike trimers. For ELISA, antigens were hydrophobically plated at 2 µg/mL and binding of human ACE2 and a set of SARS-CoV-2 antibodies was assessed. ELISA reveals that ACE2 and mAbs bind all antigens in a similar manner. Dilution series of hACE2 and mAbs starting at 10 µg/mL were bound to coated antigens. Binding was quantified using an anti-human-Fc HRP secondary. Each binding curve represents the average binding from 4 replicates and error bars are the standard deviation.



Neutralizing mAb	Determined IC ₅₀ value (µg/mL)	Literature IC ₅₀ value (µg/mL)
CB6	0.02 ± 0.009	0.036
COVA2-15	0.004 ± 0.002	0.008

Figure S6. Validation of a SARS-CoV-2 neutralization assay using a spike-pseudotyped lentivirus.

The spike pseudotyped lentivirus assay was validated using two published SARS-CoV-2 neutralizing mAbs (CB6 (58) and COVA2-15 (5)) and one SARS-CoV-2 reactive mAb known to be non-neutralizing (CR3022) (55-57). CB6 and COVA2-15 dilution curves were fit with a three-parameter non-linear regression to obtain IC₅₀ values (Methods). Neutralization assays were performed in technical duplicate or triplicate in 4 independent experiments and one representative curve is shown. Mean IC₅₀ values from replicates are shown in the table with standard deviation.

	S-Fer	ΔC-Fer	S-GCN4	ΔC-GCN4	RBD	CCP
Day 21 (Prime only)						
RBD IgG ELISA titer (EC₅₀)	3.2 ± 1.6 x 10 ³	6.0 ± 4.3 x 10 ³	2.0 ± 1.5 x 10 ³	1.3 ± 1.7 x 10 ³	3.0 ± 6.0 x 10 ³	---
Spike IgG ELISA titer (EC₅₀)	6.1 ± 3.3 x 10 ³	8.7 ± 6.5 x 10 ³	5.2 ± 2.7 x 10 ³	2.2 ± 2.6 x 10 ³	2.4 ± 1.3 x 10 ²	---
% ACE2 blocking (1:50)	33 ± 14	45 ± 18	17 ± 7.6	13 ± 15	12 ± 6.5	---
% ACE2 blocking (1:500)	0.62 ± 2.3	2.8 ± 1.8	1.4 ± 1.6	4.4 ± 3.0	1.4 ± 2.5	---
Spike-pseudotyped lentivirus neutralizing titer (IC₅₀)	1.1 ± 1.2 x 10 ³	1.6 ± 1.2 x 10 ³	1.9 ± 1.2 x 10 ²	1.2 ± 0.69 x 10 ²	1.0 x 10 ² (LOQ)	6.2 ± 6.3 x 10 ²
Day 28 (Prime + Boost)						
RBD IgG ELISA titer (EC₅₀)	2.9 ± 1.3 x 10 ⁴	8.2 ± 4.8 x 10 ⁴	7.4 ± 4.9 x 10 ⁴	5.2 ± 3.9 x 10 ⁴	9.2 ± 6.9 x 10 ⁴	---
Spike IgG ELISA titer (EC₅₀)	6.6 ± 2.5 x 10 ⁴	1.2 ± 0.66 x 10 ⁵	1.9 ± 1.2 x 10 ⁵	8.8 ± 5.9 x 10 ⁴	5.4 ± 3.6 x 10 ⁴	---
% ACE2 blocking (1:50)	94 ± 15	99 ± 0.67	96 ± 9.3	93 ± 9.4	93 ± 14	---
% ACE2 blocking (1:500)	22 ± 8.1	50 ± 23	46 ± 21	44 ± 24	61 ± 26	---
Spike-pseudotyped lentivirus neutralizing titer (IC₅₀)	1.2 ± 0.53 x 10 ⁴	3.4 ± 2.5 x 10 ⁴	8.8 ± 7.2 x 10 ³	9.4 ± 13.4 x 10 ³	1.5 ± 1.7 x 10 ⁴	6.2 ± 6.3 x 10 ²

Table S1. Mean ELISA binding titers, % ACE2 blocking, and spike-pseudotyped lentivirus neutralization titers from antigen groups at day 21 and day 28 post immunization. Each value represents the mean EC₅₀ titer (ELISA binding), the mean % ACE2 blocking, or the mean IC₅₀ titer (spike-pseudotyped lentivirus neutralization) for each antigen group at day 21 and day 28. Error represents the standard deviation.

Day 21 RBD ELISA titers

Dunn's multiple comparisons test	Mean rank diff.	Significant?	Summary	Adjusted P Value
RBD vs. ΔC-GCN4	3.200	No	<i>ns</i>	>0.9999
RBD vs. S-GCN4	-3.300	No	<i>ns</i>	>0.9999
RBD vs. ΔC-Fer	-20.70	Yes	*	0.0150
RBD vs. S-Fer	-10.70	No	<i>ns</i>	>0.9999
ΔC-GCN4 vs. S-GCN4	-6.500	No	<i>ns</i>	>0.9999
ΔC-GCN4 vs. ΔC-Fer	-23.90	Yes	**	0.0025
ΔC-GCN4 vs. S-Fer	-13.90	No	<i>ns</i>	0.3299
S-GCN4 vs. ΔC-Fer	-17.40	No	<i>ns</i>	0.0761
S-GCN4 vs. S-Fer	-7.400	No	<i>ns</i>	>0.9999
ΔC-Fer vs. S-Fer	10.00	No	<i>ns</i>	>0.9999

Day 21 Spike ELISA titers

Dunn's multiple comparisons test	Mean rank diff.	Significant?	Summary	Adjusted P Value
RBD vs. ΔC-GCN4	-13.50	No	<i>ns</i>	0.3837
RBD vs. S-GCN4	-23.20	Yes	**	0.0037
RBD vs. ΔC-Fer	-31.20	Yes	****	<0.0001
RBD vs. S-Fer	-26.10	Yes	***	0.0006
ΔC-GCN4 vs. S-GCN4	-9.700	No	<i>ns</i>	>0.9999
ΔC-GCN4 vs. ΔC-Fer	-17.70	No	<i>ns</i>	0.0663
ΔC-GCN4 vs. S-Fer	-12.60	No	<i>ns</i>	0.5326
S-GCN4 vs. ΔC-Fer	-8.000	No	<i>ns</i>	>0.9999
S-GCN4 vs. S-Fer	-2.900	No	<i>ns</i>	>0.9999
ΔC-Fer vs. S-Fer	5.100	No	<i>ns</i>	>0.9999

Day 28 RBD ELISA titers

Dunn's multiple comparisons test	Mean rank diff.	Significant?	Summary	Adjusted P Value
RBD vs. ΔC-GCN4	11.10	No	<i>ns</i>	0.8863
RBD vs. S-GCN4	3.200	No	<i>ns</i>	>0.9999
RBD vs. ΔC-Fer	0.8000	No	<i>ns</i>	>0.9999
RBD vs. S-Fer	20.40	Yes	*	0.0175
ΔC-GCN4 vs. S-GCN4	-7.900	No	<i>ns</i>	>0.9999
ΔC-GCN4 vs. ΔC-Fer	-10.30	No	<i>ns</i>	>0.9999
ΔC-GCN4 vs. S-Fer	9.300	No	<i>ns</i>	>0.9999
S-GCN4 vs. ΔC-Fer	-2.400	No	<i>ns</i>	>0.9999
S-GCN4 vs. S-Fer	17.20	No	<i>ns</i>	0.0833
ΔC-Fer vs. S-Fer	19.60	Yes	*	0.0264

Day 28 Spike ELISA titers

Dunn's multiple comparisons test	Mean rank diff.	Significant?	Summary	Adjusted P Value
RBD vs. ΔC-GCN4	-8.300	No	<i>ns</i>	>0.9999
RBD vs. S-GCN4	-22.70	Yes	**	0.0050
RBD vs. ΔC-Fer	-16.60	No	<i>ns</i>	0.1089
RBD vs. S-Fer	-4.400	No	<i>ns</i>	>0.9999
ΔC-GCN4 vs. S-GCN4	-14.40	No	<i>ns</i>	0.2718
ΔC-GCN4 vs. ΔC-Fer	-8.300	No	<i>ns</i>	>0.9999
ΔC-GCN4 vs. S-Fer	3.900	No	<i>ns</i>	>0.9999
S-GCN4 vs. ΔC-Fer	6.100	No	<i>ns</i>	>0.9999
S-GCN4 vs. S-Fer	18.30	Yes	*	0.0500
ΔC-Fer vs. S-Fer	12.20	No	<i>ns</i>	0.6129

Table S2. Statistical analysis of spike and RBD ELISA titers from day 21 and day 28 immunization timepoints. Calculated EC₅₀ values for each animal for RBD and spike at each time point were compiled by group and assessed using a Kruskal-Wallis ANOVA followed by Dunn's multiple comparisons test. Pairwise comparisons are shown.

Day 21 pseudovirus neutralization titers

Dunn's multiple comparisons test	Mean rank diff.	Significant?	Summary	Adjusted P Value
RBD vs. SΔC-GCN4	-1.750	No	ns	>0.9999
RBD vs. S-GCN4	-7.300	No	ns	>0.9999
RBD vs. SΔC-Fer	-26.80	Yes	****	<0.0001
RBD vs. S-Fer	-19.15	Yes	*	0.0122
SΔC-GCN4 vs. S-GCN4	-5.550	No	ns	>0.9999
SΔC-GCN4 vs. SΔC-Fer	-25.05	Yes	***	0.0002
SΔC-GCN4 vs. S-Fer	-17.40	Yes	*	0.0329
S-GCN4 vs. SΔC-Fer	-19.50	Yes	**	0.0099
S-GCN4 vs. S-Fer	-11.85	No	ns	0.4531
SΔC-Fer vs. S-Fer	7.650	No	ns	>0.9999

Day 28 pseudovirus neutralization titers

Dunn's multiple comparisons test	Mean rank diff.	Significant?	Summary	Adjusted P Value
RBD vs. SΔC-GCN4	5.900	No	ns	>0.9999
RBD vs. S-GCN4	2.800	No	ns	>0.9999
RBD vs. SΔC-Fer	-15.70	No	ns	0.1603
RBD vs. S-Fer	-4.000	No	ns	>0.9999
SΔC-GCN4 vs. S-GCN4	-3.100	No	ns	>0.9999
SΔC-GCN4 vs. SΔC-Fer	-21.60	Yes	**	0.0092
SΔC-GCN4 vs. S-Fer	-9.900	No	ns	>0.9999
S-GCN4 vs. SΔC-Fer	-18.50	Yes	*	0.0454
S-GCN4 vs. S-Fer	-6.800	No	ns	>0.9999
SΔC-Fer vs. S-Fer	11.70	No	ns	0.7270

Table S3. Statistical analysis of spike and RBD neutralization titers from day 21 and day 28 immunization timepoints. Calculated neutralization IC₅₀ values for each animal at each time point were compiled by group and assessed using a Kruskal-Wallis ANOVA followed by Dunn's multiple comparisons test. Pairwise comparisons are shown.

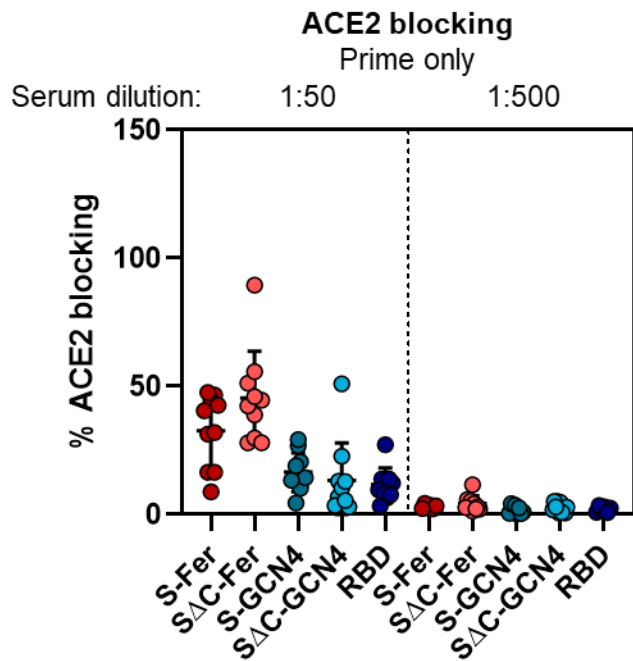
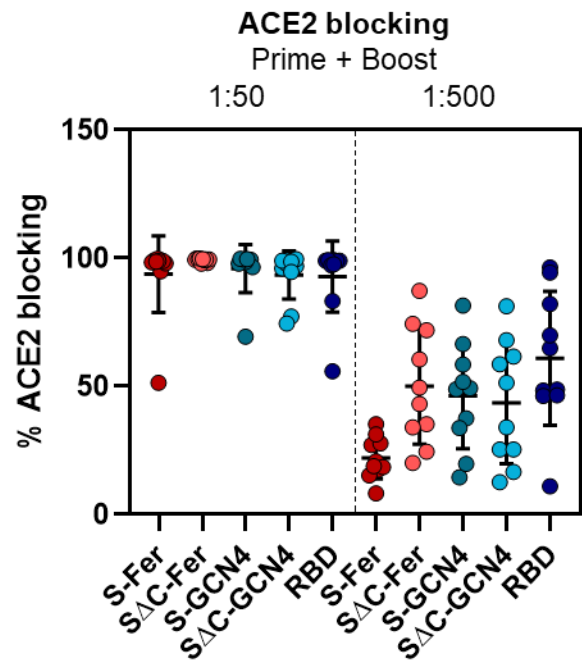
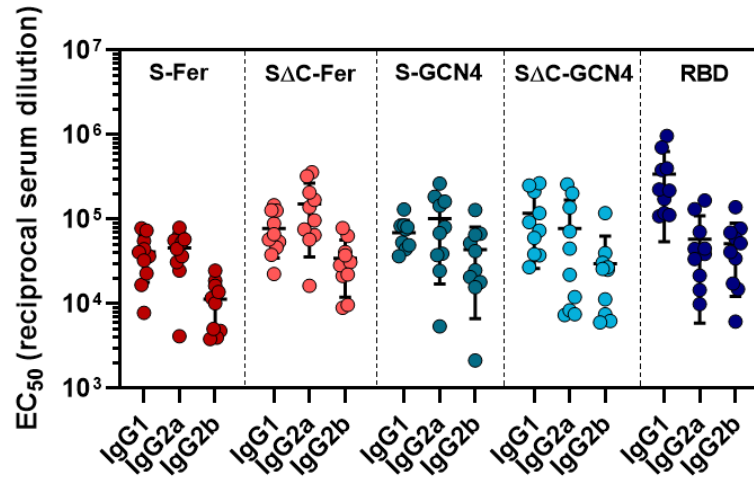
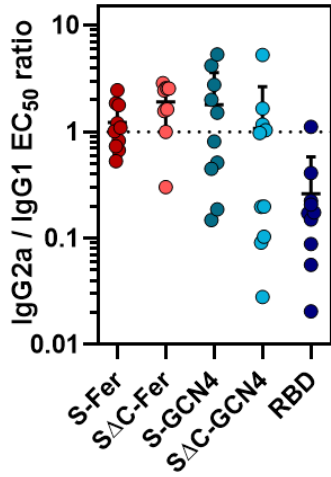
A**B**

Figure S7. Sera from mice immunized with SARS-CoV-2 block ACE2 binding to RBD, as indicated by ELISA. (A) ACE2 blocking activity of sera from mice immunized with a single dose of antigen was determined using an RBD-based ELISA in which RBD-coated plates were incubated with serum dilutions and then ACE2 binding was assayed. ACE2 blocking at a 1:50 and 1:500 serum dilution is shown for each group, and indicates that following a single dose, minimal ACE2 blocking activity is seen in the serum even at a high concentration. No groups show detectable ACE2 blocking activity in the serum diluted at 1:500. Each point represents the average % ACE2 blocking for a single animal assayed in duplicate; each bar represents the mean % ACE2 blocking from the group ($n = 10$ mice per group); error bars represent standard deviation. (B) ACE2 blocking activity was assessed after two doses of antigen and indicates a notable increase in serum antibodies capable of blocking ACE2 binding to RBD. Nearly all ACE2 binding was blocked with a 1:50 serum dilution from all groups, and all groups had detectable blocking at 1:500. Groups and error are as defined in (A).

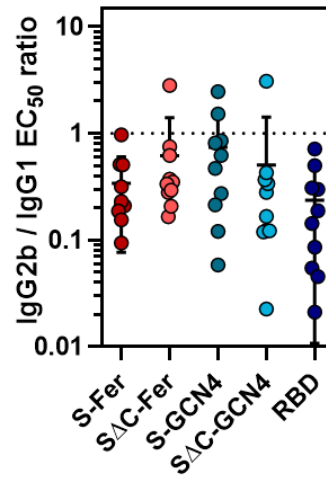
A



B



C



D

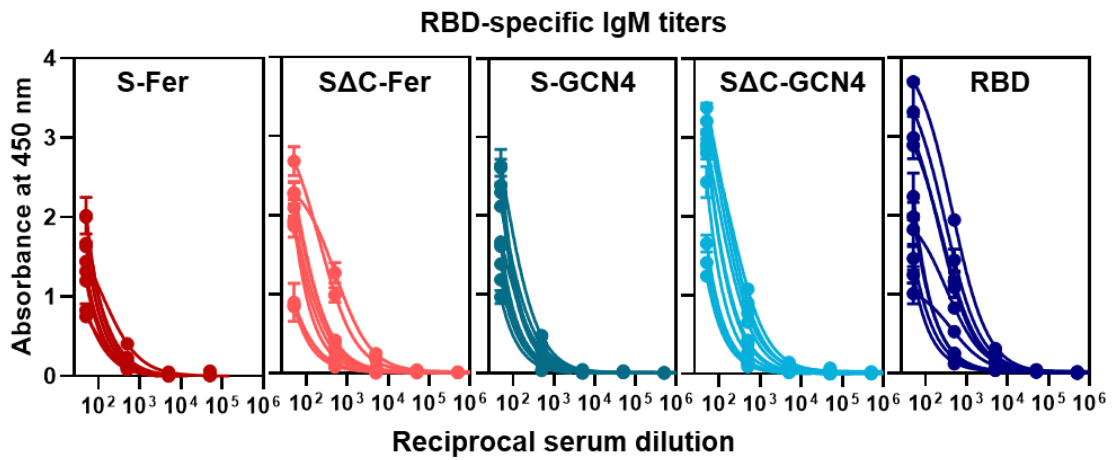
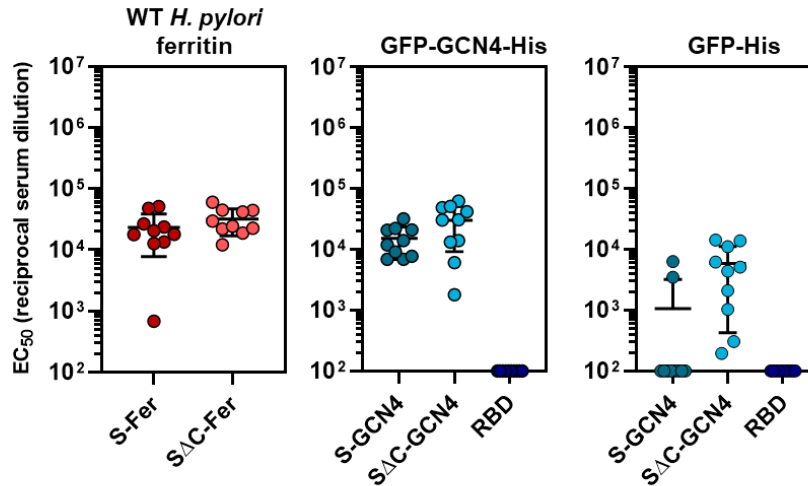


Figure S8. Immunization with SARS-CoV-2 antigens adjuvanted with Quil-A/MPLA leads to robust RBD-specific IgG1 and IgG2 isotype responses and minimal levels of IgM following two doses. (A) ELISA binding titers quantifying RBD-specific IgG1, IgG2a, and IgG2b subclass responses following two doses of antigen demonstrate broad IgG subclass elicitation with varied ratios among different antigen groups. Each point represents the EC_{50} titer from a single animal; each bar represents the mean EC_{50} titer from the group ($n = 10$ mice per group); error bars represent standard deviation. (B) Ratios of RBD-specific IgG2a/IgG1 following two doses of antigen for each group. S Δ C-Fer and S-GCN4 groups exhibit higher IgG2a responses as compare to IgG1, whereas S-Fer and S Δ C-GCN4 groups exhibit roughly balanced levels and the RBD group exhibits substantially greater IgG1 response. Each point represents the EC_{50} ratio from a single animal; each bar represents the mean EC_{50} ratio from the group ($n = 10$ mice per group); error bars represent standard deviation. (C) Ratios of RBD-specific IgG2b/IgG1 following two doses of antigen for each group. All groups exhibit mean IgG2b/IgG1 ratios less than 1, indicating a lower IgG2b response as compared to IgG1. Groups and error are as defined in (B). (D) RBD-specific IgM titers following two doses of antigen indicates lower levels of IgM as compared to IgG titers. Each curve represents an experimental replicate from each animal ($n = 10$ mice per group); error bars represent standard deviation for each point.



	S-Fer	ΔC-Fer	S-GCN4	ΔC-GCN4	RBD
WT <i>H. pylori</i> ferritin ELISA titers (EC ₅₀)	2.3 ± 1.6 × 10 ⁴	3.2 ± 1.5 × 10 ⁴	---	---	---
GFP-GCN4-His ELISA titers (EC ₅₀)	---	---	1.5 ± 0.84 × 10 ⁴	3.0 ± 2.1 × 10 ⁴	1.0 × 10 ² (LOQ)
GFP-His ELISA titers (EC ₅₀)	---	---	1.1 ± 2.1 × 10 ³	5.9 ± 5.4 × 10 ³	1.0 × 10 ² (LOQ)

Figure S9. Off-target antibody responses to either *H. pylori* ferritin or GCN4-trimerization domain are similar between ferritin and trimer immunization groups. ELISA binding titers against non-SARS-CoV-2 antigen domains following two doses of antigen reveal off-target responses that are similar or less than antigen-specific RBD and spike titers (see Figure 4D and Table S1). Each point represents the EC₅₀ ratio from a single animal; each bar represents the mean EC₅₀ ratio from the group ($n = 10$ mice per group); error bars represent standard deviation. Points with signal less than EC₅₀ 1:100 dilution are placed at the limit of quantitation for the assay. Values shown in table correspond to mean titers for each group and error represents standard deviation.

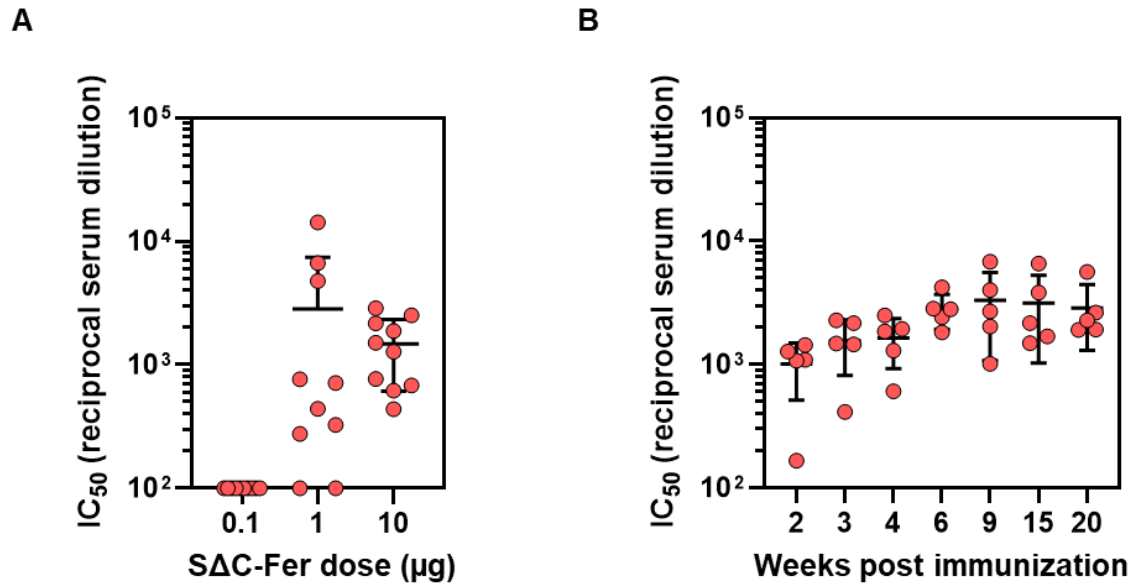


Figure S10. Immunization with SΔC-Fer leads to a dose-dependent neutralizing antibody response and elicits neutralizing antibody levels that are stable up to 20 weeks post immunization. (A) Neutralizing antibody responses against SΔC-Fer show dose-dependent trends. Mice ($n = 10$ per dose) were immunized with a single dose of either 0.1 μg , 1 μg , or 10 μg SΔC-Fer particles adjuvanted with 10 μg Quil-A / 10 μg MPLA via subcutaneous injection. Serum was collected at day 28 post immunization and analyzed for spike-pseudotyped lentivirus neutralization activity. Each point represents the IC₅₀ titer from a single animal; each bar represents the mean IC₅₀ titer from each group; error bars represent the standard deviation. Samples with neutralizing activity that was undetectable at 1:50 dilution or with an IC₅₀ less than 1:100 dilution are placed at the limit of quantitation. (B) Neutralizing antibody responses increase between 2- and 6-weeks post immunization with 20 μg SΔC-Fer and remain stable to 20-weeks post immunization. Mice ($n = 5$) were immunized with a single dose of 20 μg SΔC-Fer particles adjuvanted with 10 μg Quil-A / 10 μg MPLA via subcutaneous injection. Serum was assessed at timepoints between 2- and 20-weeks post immunization for neutralization of spike-pseudotyped lentivirus. Groups and error are as described in (A).